

MRI features of primary rare malignancies of the liver: A report from four university centres

Richard C. Semelka¹ · Nadesan Nimojan¹ · Saman Chandana¹ · Miguel Ramalho² · Suzanne L. Palmer³ · Danielle DeMulder⁴ · Carolina Parada Villavicencio⁵ · John Woosley⁶ · Bonnie L. Garon³ · Reena C. Jha⁴ · Frank H. Miller⁵ · Ersan Altun¹

Received: 22 February 2017 / Revised: 12 September 2017 / Accepted: 27 September 2017 / Published online: 27 October 2017
© European Society of Radiology 2017

Abstract

Purpose To determine if rare primary malignancies of the liver may have consistent features on magnetic resonance imaging (MRI).

Materials and methods This IRB-compliant retrospective study reviewed the records from the pathology departments of four university centres over an 11-year period from 2005–2016 to identify rare primary malignant tumours, which were cross-referenced with MRI records. MRI studies of these patients were reviewed to determine if these tumours exhibited consistent and distinctive features.

Results Sixty patients were identified with rare primary liver tumours. The following distinctive features and frequency of occurrence were observed: mixed hepatocellular carcinoma-cholangiocarcinoma showed regions of wash-out in 7/19 of patients; 6/6 of fibrolamellar carcinomas demonstrated large heterogeneous lesions with large heterogeneous central scars; epithelioid haemangiopericytoma larger than 2 cm showed

target-like enhancement in late-phase enhancement in 9/13; sarcomas excluding angiosarcoma had central necrosis in 3/9 and haemorrhage in 5/9; angiosarcomas showed centripetal progressive nodular enhancement in 3/6 and showed regions of haemorrhage in 3/6; and 7/7 of primary hepatic lymphomas showed encasement of vessels.

Conclusion Although helpful features for the differentiation of rare primary malignancies of the liver are identified, no MRI features appear to be specific and therefore histopathological confirmation is usually required for definitive diagnosis.

Key points

- No MRI features appear to be specific for rare primary liver malignancies.
- Haemorrhage is a helpful sign in diagnosis of primary hepatic sarcomas.
- Angiosarcomas may show progressive nodular enhancement towards the centre mimicking haemangioma.
- Vessel encasement is a helpful sign in diagnosis of primary hepatic lymphoma.

✉ Ersan Altun
ersan_altun@med.unc.edu

¹ Department of Radiology, University of North Carolina at Chapel Hill, 101 Manning Drive, Chapel Hill, NC 27514, USA

² Department of Radiology, Hospital Garcia de Orta, EPE, Almada, Portugal

³ Department of Radiology, University of South California, Los Angeles, CA, USA

⁴ Department of Radiology, Georgetown University, Washington, DC, USA

⁵ Department of Radiology, Northwestern University, Chicago, IL, USA

⁶ Department of Pathology, University of North Carolina at Chapel Hill, Chapel Hill, NC, USA

Keywords Magnetic resonance imaging · Epithelioid haemangiopericytoma · Fibrolamellar hepatocellular carcinoma · Sarcoma · Lymphoma

Abbreviations

AS	Angiosarcoma
CCA	Cholangiocarcinoma
EHE	Epithelioid haemangiopericytoma
FL	Fibrolamellar hepatocellular carcinoma
HCC	Hepatocellular carcinoma
PHL	Primary hepatic lymphoma

Introduction

Among primary malignant tumours, hepatocellular carcinomas (HCCs) are responsible for 80–85 % of primary malignant tumours [1, 2], followed by intrahepatic cholangiocarcinomas (CCAs), which account for 9.7 % [1, 2]. Mixed HCC-CCA, mesenchymal tumours, such as angiosarcoma (AS) and epithelioid haemangioma (EHE), primary hepatic lymphoma (PHL), fibrolamellar hepatocellular carcinoma (FL) and other sarcomas are rare, accounting for the remaining 1.1 % of primary hepatic neoplasms [1, 2].

Magnetic resonance imaging (MRI) is a highly accurate method for evaluating focal liver lesions, and specific features of common lesions are usually diagnostic for these entities including but not limited to HCC, haemangiomas and focal nodular hyperplasia (FNH) [1]. However, biopsy is still used for common types of focal liver lesions with atypical imaging features and for rare types of focal liver lesions.

Although there are multiple studies about MRI features of rare primary liver tumours in the literature [3–8], the number of studies comparing MRI features of these tumours in a single cohort is limited [9, 10]. Additionally, heterogeneity of study populations in these single-cohort studies was another limiting factor, which necessitates further studies to be performed in order to obtain reproducible results.

Therefore, the purpose of our study was to pool the experience of multiple university centres in order to determine if these rare malignancies show features that may be consistent or even diagnostic for these entities.

Materials and methods

Study population

This multicentre, retrospective study was performed after each institutional review board approval, with waiver of the informed consent requirement. The study was performed in compliance with the Health Insurance Portability and Accountability Act.

Four university centres reviewed the Pathology records over an 11-year period from 1 January 2005 to 1 January 2016 to identify rare primary malignancies of the liver in patients over 15 years of age. This data was cross-referenced with records of the MRI centres to identify lesions that also had been imaged by MRI prior to any intervention. For study inclusion, all lesions were evaluated by MRI at initial presentation without prior treatment. HCCs, CCAs and hepatoblastomas were excluded. However, no hepatoblastomas were identified in our pooled populations over 15 years of age.

Our study population included 60 consecutive patients (31 females, 29 males; mean age, 51.1 ± 18.1 years). The following malignancies were identified in decreasing order of

frequency: mixed HCC-CCA (19 patients, 31.6 %), EHE (13 patients, 21.6 %), liver sarcoma excluding AS (nine patients, 15 %), PHL (seven patients, 11.6 %), FL (nine patients, 10 %) and AS (six patients, 10%).

MRI technique

All MRI studies were performed on high-field MRI systems including 1.5 Tesla (T) and 3.0T at one of four university medical centres (University Medical Centres A–D). The details and specific parameters of the representative MRI protocols are given in Table 1. Serial dynamic contrast-enhanced imaging was performed on the late arterial (at 35–40 s after the contrast injection with empirical timing or scanning time based on fluoroscopy preparation timing sequence), portal venous (between 45–90 s after the contrast injection) and equilibrium phases (between 2–5 min after the contrast injection) with gadolinium-based contrast agents, including gadobenate dimeglumine (MultiHance®; Bracco Diagnostics Inc., Princeton, NJ, USA) (0.05–0.1 mmol/kg), gadodiamide (Omniscan®; GE Healthcare, Oakville, Ontario, Canada) (0.1 mmol/kg), gadopentate dimeglumine (Magnevist®; Bayer Healthcare Pharmaceuticals Inc., Wayne, NJ, USA) (0.1 mmol/kg), gadobutrol (Gadavist®; Bayer Healthcare Pharmaceuticals Inc., Wayne, NJ, USA) (0.1 mmol/kg) and gadoterate meglumine (Dotarem®, Guerbet LLC; Bloomington, IN, USA) (0.1 mmol/kg). All contrast agents were injected with specific doses stated above followed by a 20-ml saline flush (2 ml/s) with a power injector. MRI examinations of all patients included in the study had acceptable image quality.

Image analysis

Individual spreadsheets were sent to each institution for qualitative MRI evaluation of each patient and included predetermined standard findings as follows: age; gender; presence of chronic liver disease; size; signal intensity on non-fat-suppressed T1-weighted images and signal intensity on fat-suppressed T2-weighted images; enhancement characteristics, vascularity; presence of scar, capsular retraction, necrosis or haemorrhage; and mass effect (i.e. displacing or encasing liver vessels). Enhancement characteristics on the late hepatic arterial phase include: (i) diffuse or focal homogeneous versus heterogeneous increased enhancement; (ii) rim type of increased enhancement; and (iii) relatively decreased enhancement compared to the background liver. Enhancement characteristics on the portal venous phase and/or equilibrium phase include: (i) washout; (ii) fading; (iii) diffuse/focal homogeneous versus heterogeneous increased enhancement; (iv) progressive increased enhancement towards the centre with or without peripheral washout (target-like enhancement); and (v) relatively decreased enhancement compared to the background liver.

Table 1 MRI imaging sequences and parameters

MR Sequence	Imaging planes	Fat suppression	Intravenous contrast material protocol	TR/TE (ms)	Flip angle (degrees)	Section thickness (mm) / Gap (%)	Matrix size	FOV
1.5 T								
Breathing dependent protocol								
T2-weighted half-Fourier RARE	Coronal, Transverse	Used, not used	Pre-contrast images	1,500 / 85	180	6 / 20 %	192 x 256	350–400
T1-weighted 2D-GRE*	Coronal, Transverse	Used, not used	Pre-contrast images	170 / 2.2–4.4	70	6 / 20 %	192 x 256	350–400
T1-weighted 3D-GRE	Coronal, Transverse	Used	Pre and Postcontrast images	3.8 / 1.7	10	3 / -	160 x 256	350–400
MRCP								
T2 Single Fast Spine Echo 2D Slab	Coronal, Oblique Coronal	Used	Pre-contrast images	2,000 / 700	180	50 / NA	224 x 384	300
T2 Fast Spin Echo 3D MRCP	Oblique Coronal	Used	Pre-contrast images	2,500 / 700	Variable	1 / -	380 x 340	350
T2-weighted half-Fourier RARE	Coronal, Oblique Coronal, Transverse	Used	Pre-contrast images	1,500 / 99	150	3 / -	240 x 256	300
3.0 T								
Breathing dependent protocol								
T2-weighted half-Fourier	Coronal, Transverse	Used, not used	Pre-contrast images	2,000 / 95	150	6 / 20 %	204 x 256	350–400
T1-weighted 2D-GRE*	Coronal, Transverse	Used, not used	Pre-contrast images	170 / 1.6–2.5	70	6 / 20 %	192 x 320	350–400
T1-weighted 3D-GRE	Coronal, Transverse	Used, not used	Pre and Postcontrast images	3.3 / 1.2	10	3 / -	204 x 256	350–400
MRCP								
T2-weighted Single Shot Echo Train Spin Echo	Coronal, Oblique Coronal	Used	Pre-contrast images	5,000 / 700	180	50	224 x 384	300
T2 Fast Spin Echo 3D MRCP	Oblique Coronal	Used	Pre-contrast images	2,400 / 700	Variable	1 / -	380 x 380	380
T2-weighted half-Fourier RARE	Coronal, Oblique Coronal, Transverse	Used	Pre-contrast images	1,500 / 99	150	3 / -	240 x 256	300

*In-phase and out-of-phase T1-weighted 2D-GRE images were acquired

Table 2 Characteristics of patient groups according to different tumour types

	Number of patients (%) (male/female)	Age range / mean (years)	Number of patients with chronic liver disease	Solitary versus multiple tumours	Tumour size range / mean (cm)
Mixed hepatocellular carcinoma-- cholangiocarcinoma	19 / 60 (31.6 %) (11/8)	20–87 / 63	14	18/1	1.3–10.9 / 4.94
Fibrolamellar hepatocellular carcinoma	6 / 60 (10 %) (2/4)	16–30 / 20.3	0	6/0	4.0–14.5 / 10
Epitheloid haemangioendothelioma	13 / 60 (21.6 %) (3/10)	29–64 / 43.3	1	2/11	1.1–4.2 / 2.7
Sarcomas excluding angiosarcoma*	9 / 60(15 %) (5/4)	17 – 73 / 51.8	0	9/0	1.8–12.8 / 11.7
Angiosarcoma	6 / 60 (10 %) (5/1)	44–73 / 60	2	2/4	1–14.3 / 7.8
Primary hepatic lymphoma	7 / 60(11.6 %) (3/4)	42–80 / 56.8	1	4/3	2–15 / 6.9

*Undifferentiated embryonal sarcoma was detected in one male (23 years old) and one female (17 years old) patient. Leiomyosarcoma was detected in a 53-year-old female. Histiocytic sarcoma was detected in a 73-year-old female. Uncharacterised sarcoma was detected in five patients (four males and one female) with an age range of 55–69 years

Based on these predetermined findings, image interpretation was performed retrospectively and blindly in consensus by two experienced board-certified reviewers at each centre for the liver lesions.

In patients who had multiple lesions showing similar morphological features, the evaluation was performed for the largest lesion. If there were more than one type of lesion that were separate from each other and with different morphological features in the liver, the largest of each type of lesion was evaluated.

Statistical analysis

A Chi-square test was applied in order to test the statistical significance of each image characteristic between different

tumour types. Values of $p < 0.05$ were considered statistically significant. All statistical analyses were performed using IBM SPSS Statistics for Mac OS X (Version 22; IBM Corp., Armonk, NY, USA).

Results

Six different types of tumours were identified in our study population. Characteristics of patient subgroups according to different tumour types is summarised in Table 2. MRI features of these different tumours including pre-contrast signal characteristics and post-gadolinium enhancement characteristics with additional morphological features are summarised in Tables 3 and 4, respectively.

Table 3 Pre-contrast signal characteristics of different tumour types

	T1 signal hyperintense / hypointense / isointense / mixed	T1 hypointensity mild / moderate to marked	T2 signal Hyperintense / hypointense / isointense / mixed	T2 signal hyperintensity mild / moderate to marked	Pre-contrast homogeneity / heterogeneity
Mixed hepatocellular carcinoma - cholangiocarcinoma (n=19)	0 / 16 / 3 / 0	4 / 12	18 / 1 / 0 / 0	9 / 9	4 / 15
Fibrolamellar hepatocellular carcinoma (n=6)	0 / 6 / 0 / 0	2 / 4	6 / 0 / 0 / 0	3 / 3	0 / 6
Epitheloid haemangioendothelioma (n=13)	0 / 13 / 0 / 0	5 / 8	13 / 0 / 0 / 0	2 / 11	1 / 12
Sarcoma excluding angiosarcoma (n=9)	0 / 8 / 0 / 1	1 / 8	9 / 0 / 0 / 0	1 / 8	1 / 8
Angiosarcoma (n=6)	1 / 2 / 0 / 3	2 / 3	6 / 0 / 0 / 0	2 / 4	0 / 6
Primary hepatic lymphoma (n=7)	0 / 6 / 1 / 0	2 / 4	7 / 0 / 0 / 0	3 / 4	5 / 2

Table 4 Post-gadolinium enhancement characteristics of different tumour types with additional morphological features including scar, necrosis and haemorrhage

	Late arterial enhancement	Portal and equilibrium phase enhancement	Homogeneous vs. heterogeneous enhancement	Scar	Necrosis	Haemorrhage
Mixed hepatocellular carcinoma - cholangiocarcinoma	Avid diffuse heterogeneous (7/19) Mild diffuse heterogeneous or rim type (11/19) Slight enhancement with relatively lower enhancement compared to the background (1/19)	Partial or complete Washout (7/19) Progressive or persistent enhancement (11/19) Fading (1/19)	0/19	0/19	3/19	0/19
Fibrolamellar hepatocellular carcinoma	Diffuse heterogeneous enhancement (6/6)	Persistent and progressive enhancement (5/6) Partial and complete Washout (1/6)	0/6	6/6	0/6	0/6
Epitheloid haemangioendothelioma	Rim type of enhancement (12/13) Mild central enhancement (1/13)	Progressive enhancement towards the centre (9/13) Persistent peripheral enhancement (2/13) Fading (1/13) Slight enhancement with relatively lower enhancement compared to the background (1/13)	1/12	0/13	0/6	0/6
Sarcomas excluding angiosarcoma	Mild peripheral enhancement (2/9) Diffuse heterogeneous enhancement (3/9) Heterogeneous peripheral enhancement (4/9)	Progressive heterogeneous and septal-like enhancement towards the centre (2/9) Progressive diffuse heterogeneous enhancement (6/9) Persistent peripheral enhancement (1/9)	1/8	0/9	3/9	5/9
Angiosarcoma	Heterogeneous peripheral enhancement (5/6) Diffuse heterogeneous enhancement (1/6)	Progressive nodular enhancement toward the centre (3/6) Heterogeneous persistent enhancement (3/6)	0/6	0/6	1/6	3/6
Primary hepatic lymphoma	Mild diffuse contrast enhancement (6/7) No enhancement (1/6)	Progressive diffuse enhancement (6/7) Fading (1/7)	3/4	0/6	0/7	0/7

Mixed hepatocellular carcinoma-cholangiocarcinoma (Fig. 1)

Nineteen patients (19/60) were identified with mixed HCC-CCA. Mixed HCC-CCA is more commonly seen in patients with cirrhosis with a statistically significant difference (Chi square = 22.3143, $p < 0.0001$). Mixed HCC-CCA were described as the tumours with: (i) the presence of two components without a transition area, (ii) the presence of two components with areas of transition, and (iii) features of both fibrolamellar variant of HCC and cholangiocellular differentiation throughout without separate areas of one or the other according to Goodman [11] and WHO [12] classifications. Of these 19 patients, 18 patients had solitary tumours with both HCC and CCA components and one patient had separate adjacent contiguous foci of HCC and CCA, which was

seen as a single tumour. The majority of patients showed diffuse heterogeneous enhancement on the late arterial phase, with avid enhancement in 37 % (7/19), and mild and peripheral enhancement in 58 % (11/19). Washout on the later phases was detected in 37 % (7/19) of the patients, and the presence of washout was significantly more common in mixed HCC-CCA compared to other primary liver lesions (Chi square = 8.048, $p = 0.0046$). Capsule was detected in 31.6 % (6/19) of the patients on the later phases.

Fibrolamellar hepatocellular carcinoma (Fig. 2)

Six patients (6/60) were identified with FL. All tumours showed a large central scar. Compared to other rare primary liver tumours, the central scar was significantly more common in FL (Chi square = 35.4006, $p < 0.0001$).

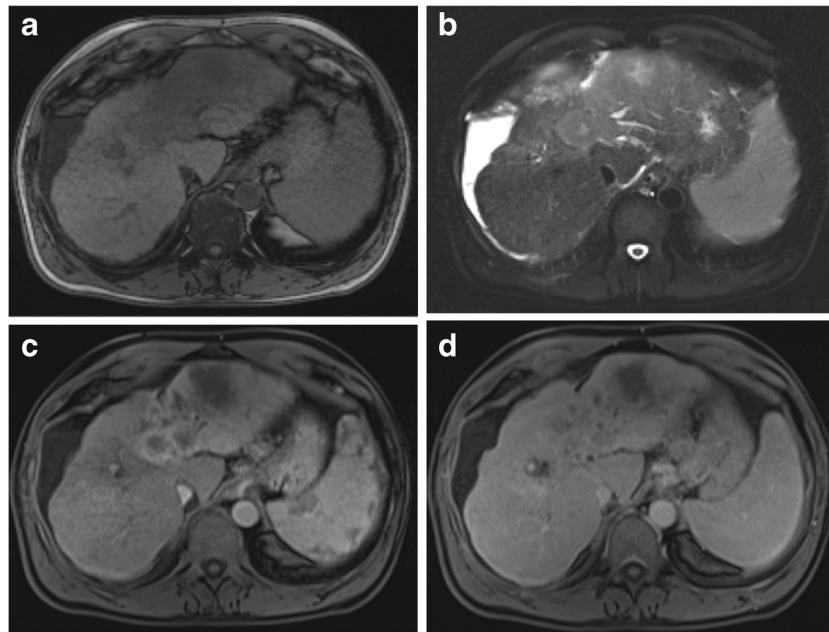


Fig. 1 Mixed HCC cholangiocarcinoma in a 61-year-old male. Transverse T1-weighted out-of-phase two-dimensional gradient echo (a), T2-weighted fat-suppressed single-shot echo train spin echo (b), post-gadolinium fat-suppressed T1-weighted three-dimensional gradient echo late hepatic arterial phase (c) and equilibrium phase (d) images. Pre-

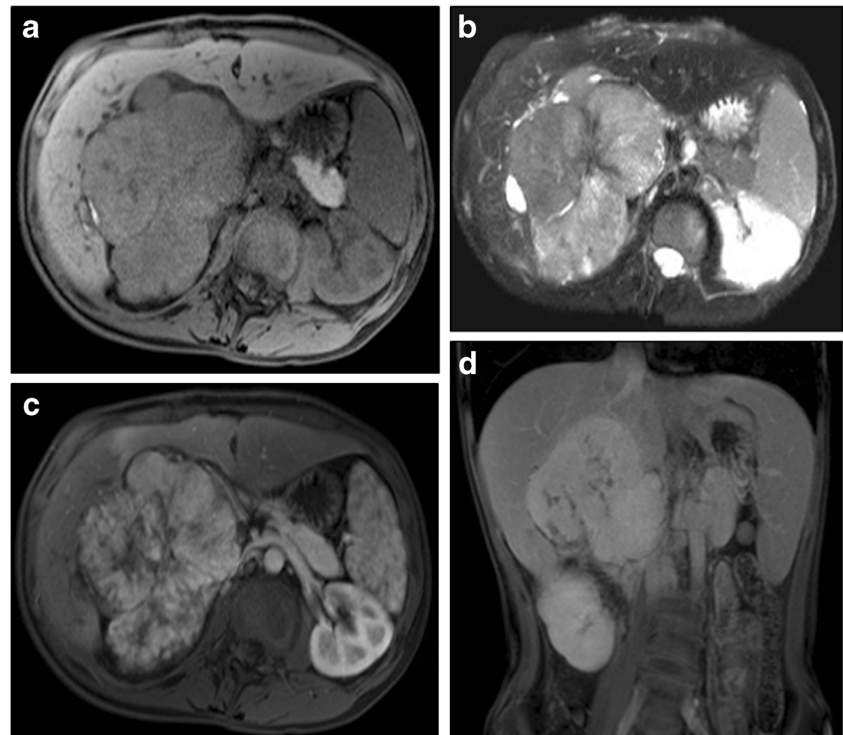
contrast images (a, b) demonstrate a centrally necrotic heterogeneous ill-defined mass predominantly in the left lobe of a cirrhotic liver. Post-gadolinium late arterial phase image (c) shows diffuse moderately intense heterogeneous enhancement. Post-gadolinium equilibrium phase image (d) shows areas of washout and areas of progressive enhancement

Central scar was large and heterogeneous on most sequences, with regions of low signal on T2 in all cases. While central scar showed no enhancement on the late arterial phase in all lesions, its enhancement was noted in 2/6 patients on the later phases.

Epithelioid haemangi endothelioma

Thirteen patients (13/60) were identified with EHE. Twelve patients (92 %) did not have underlying chronic liver disease. The lesions were larger than 2 cm in 11/13 patients and the majority

Fig. 2 Fibrolamellar hepatocellular carcinoma in a 16-year-old male. Transverse T1-weighted fat-suppressed three-dimensional (3D) gradient echo (GRE) (a), T2-weighted fat-suppressed single-shot echo train spin echo (b), post-gadolinium fat-suppressed T1-weighted late hepatic arterial phase (c) and equilibrium phase 3D GRE (d) images. A large heterogeneous tumour with a T2 hypointense large central radiating scar is seen on pre-contrast images (a, b). On the late arterial phase image (c), the tumour exhibits diffuse moderate heterogeneous enhancement with negligible enhancement of large radiating scar. On delayed phase image (d), the tumour remains moderately hyperintense to background liver, and portions of central scar enhance



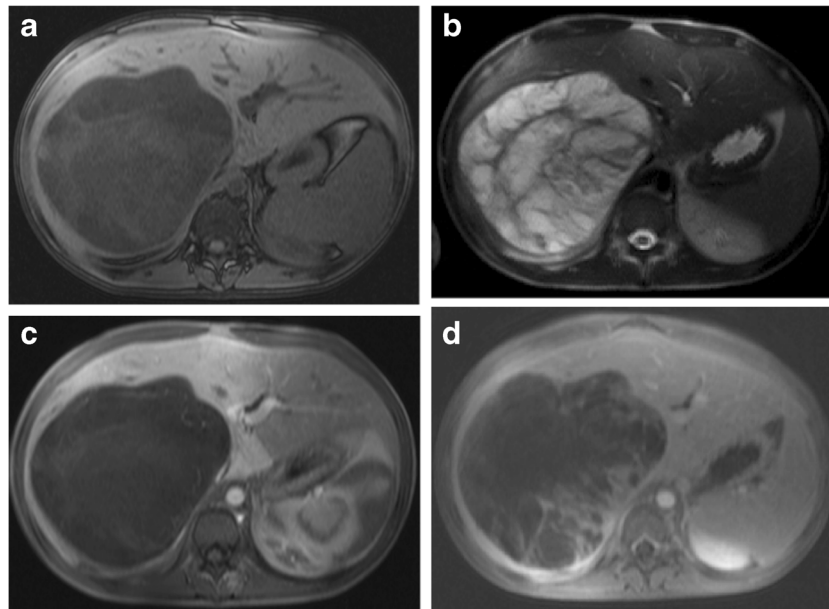


Fig. 3 Undifferentiated embryonal sarcoma in a 17-year-old female. Transverse T1-weighted fat-suppressed three-dimensional (3D) gradient echo (GRE) (a), T2-weighted fat-suppressed single-shot echo train spin echo (b), post-gadolinium fat-suppressed T1-weighted late hepatic arterial phase (c) and equilibrium phase (d) 3D GRE images. A large

heterogeneous mass lesion with high fluid content shows areas central high T1 signal, which is suggestive of haemorrhage (a, b). The tumour shows mild peripheral enhancement on the late arterial phase (c) and centrally progressive heterogeneous enhancement with septal enhancement on the later phases

of them demonstrated moderately low T1 and moderately high T2 signal on pre-contrast images. Target-like enhancement, which is characterised by delayed progressive enhancement towards the centre, was detected in 69 % (9/13) of the patients and all of these were larger than 2 cm. The lesions predominantly were located in subcapsular locations and were associated with capsular retraction in 61.5 % (8/13) of the patients.

Sarcomas excluding angiosarcoma

Nine patients (9/60) with sarcoma were identified; they were subcategorised as: undifferentiated embryonal sarcoma (n=2) (Fig. 3), leiomyosarcoma (n=1) (Fig. 4), malignant histiocytosarcoma (n=1) and uncharacterised hepatic sarcomas (n=5).

Fig. 4 Leiomyosarcoma of the liver in a 53-year-old female. Transverse T1-weighted fat-suppressed three dimensional (3D) gradient echo (GRE) (a), T2-weighted fat-suppressed single-shot echo train spin echo (b), post-gadolinium fat-suppressed T1-weighted late hepatic arterial phase (c) and portal venous phase 3D GRE (d) images. A large heterogeneous mass with central necrosis is seen on pre-contrast images (a, b). Diffuse heterogeneous enhancement is noted on the late arterial phase (c) with progression of the enhancement towards the centre on the later phases (d). No enhancement is noted at the necrotic centre

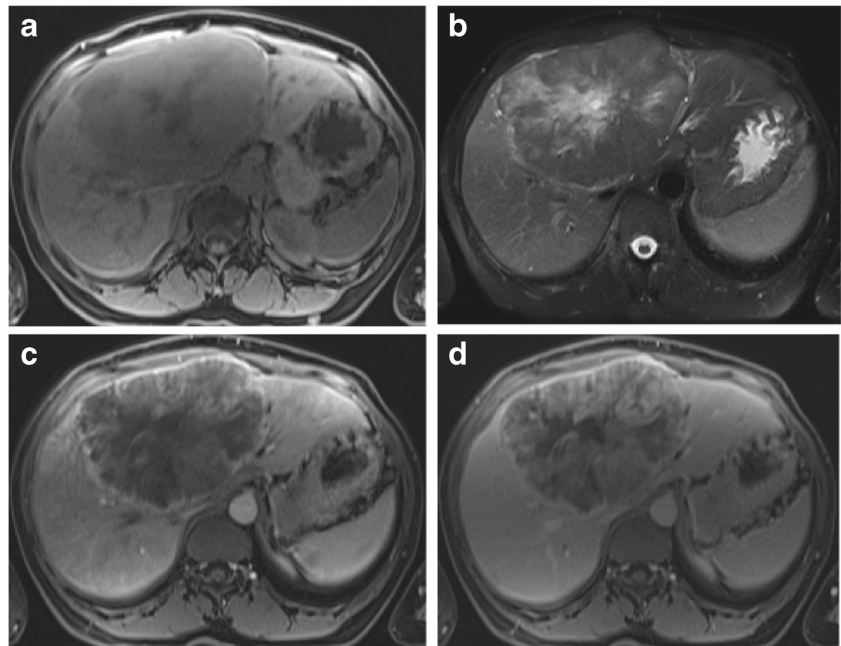
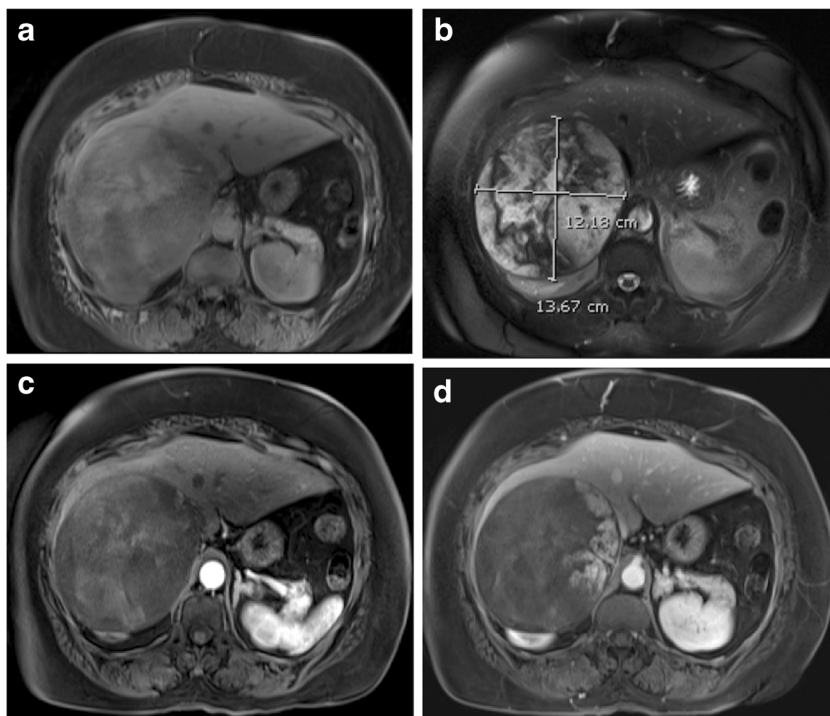


Fig. 5 Angiosarcoma in a 71-year-old female. Transverse T1-weighted fat-suppressed three-dimensional (3D) gradient echo (GRE) (a), T2-weighted fat-suppressed single-shot echo train spin echo (b), post-gadolinium fat-suppressed T1-weighted late hepatic arterial phase (c) and equilibrium phase 3D GRE (d) images. Pre-contrast images (a, b) show heterogeneous round large mass with mixed signal, which is suggestive of haemorrhage. Late arterial phase image (c) shows minimal peripheral enhancement and portal venous phase image (d) shows centripetal progressive nodular enhancement. The centripetal progressive enhancement mimics the appearance of a haemangioma



Undifferentiated embryonal sarcomas (n=2) had high fluid content and cystic spaces and therefore showed mild peripheral enhancement on the late arterial phase and progressive heterogeneous and septal-like enhancement on the later phases. Internal haemorrhage was detected in undifferentiated embryonal sarcomas (n=2) and uncharacterised hepatic sarcomas (n=3). Internal haemorrhage (5/9) was significantly more common in sarcomas excluding angiosarcomas compared to other lesions including angiosarcomas (Chi square = 5.301, $p = 0.0213$). Central necrosis was detected in leiomyosarcoma (n=1) and uncharacterised hepatic sarcomas (n=2).

Angiosarcoma (Fig. 5)

Six patients (6/60) with AS were identified. Progressive nodular enhancement towards the centre mimicking haemangiomas were noted in 3/6 patients. Intratumoral haemorrhage was seen in three patients (50 %, 3/6) and the haemorrhage was significantly more common in angiosarcomas compared to other lesions including other sarcomas (Chi square = 4.6314, $p = 0.0314$).

The presence of haemorrhage was significantly more common in all types of sarcomas compared to other lesions (Chi square = 15.5769, $p < 0.0001$).

Primary hepatic lymphoma (Fig. 6)

Seven patients (7/60) were identified with PHL. Post-gadolinium minimal enhancement or no enhancement on the

late arterial phase and mild late enhancement on the later phases were detected without evidence of necrosis in all our cases. Tumour masses encased the vessels rather than displacing them, which was observed in all cases of primary hepatic lymphoma in our study. This feature was significant for primary hepatic lymphoma (Chi square = 50.6888, $p < 0.0001$) and was not seen in other liver lesions.

Discussion

Overall, underlying chronic liver disease was either rare or absent in all tumour types except mixed HCC-CCA in our patient group, and this is in agreement with the literature since chronic liver disease is a risk factor for HCC-CCA [13].

Mixed hepatocellular carcinoma–cholangiocarcinoma

Previously described dynamic MR features [13–15] concurred with our findings. Prior reports by Fowler et al. [13] and Maximina et al. [14] described similar features of signal intensity as we describe herein. Both of these studies described ring enhancement as a common feature. De Campos et al. [15] also showed ring enhancement in a significant number of patients (> 50 %) on late arterial phase. In addition to ring enhancement, the presence of heterogeneous enhancement on late arterial phase was also described in prior studies [15]. Maximinia et al. [14] and De Campos et al. [15] also described partial washout in these types of tumours on the later phases,

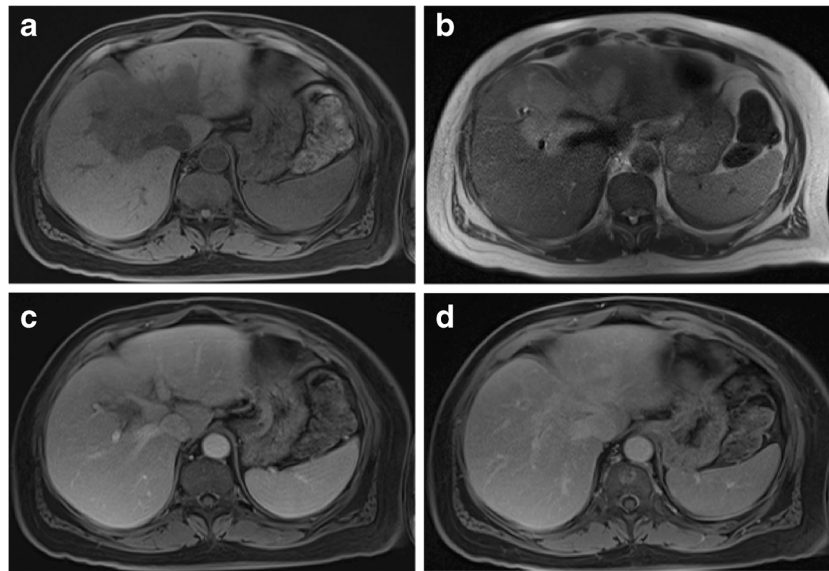


Fig. 6 Primary hepatic lymphoma in a 60-year-old male. Transverse T1-weighted fat-suppressed three-dimensional (3D) gradient echo (GRE) (a), T2-weighted single-shot echo train spin echo (b), post-gadolinium fat-suppressed T1-weighted late hepatic arterial phase (c) and equilibrium

phase 3D GRE (d) images. The lesion shows homogeneous moderately low T1 and mildly high T2 signal on pre-contrast images (a, b). The late arterial (c) and portal venous phase images (d) show diffuse mild enhancement with no necrosis. The lesion encases the vessels

whereas Fowler et al. [13] did not specifically mention partial washout. Additionally, the presence of progressive delayed enhancement was also a common feature [13–16].

In a significant number of patients these tumours can mimic both HCC and CCA. Recently, it has been reported that imaging features including peripheral rim enhancement, portal venous and delayed phase progressive central enhancement, peripheral washout, capsular retraction, diffusion restriction and biliary dilatation are helpful for the diagnosis of mixed HCC-CCA [3, 16]. The use of gadoxetic acid-enhanced MRI may be helpful for the differentiation of the CCA component from the HCC component in these mixed tumours, although its role in the diagnosis of mixed HCC-CCA has not been determined yet [17].

Fibrolamellar hepatocellular carcinoma

Distinction between FL and conventional HCC, and from certain benign liver masses, especially FNH is critical since central scar may be seen in these entities. As shown in our study, central scar was virtually present and the scar was large and heterogeneous on most sequences, with regions of low signal on T2, which classically distinguishes them from FNH, which has a small central scar that demonstrates homogeneous signal behaviour, and generally high signal intensity on T2 [2, 18, 19]. Additionally, central scars in conventional HCCs usually demonstrate high T2 signal [2]. In all cases, the scar did not show enhancement on the late hepatic arterial phase and in 75 % [4/6] of cases on the later phases in our patient group. This is also a

common finding that concurs with the literature [2, 20]. Diffuse heterogeneous enhancement on the arterial phase was detected in all patients, distinguishing itself from diffuse homogeneous enhancement with FNH [2].

Epitheloid haemangi endothelioma

Four prior MRI reports have described EHE [21–24]. MRI features in the four prior studies and our own share common elements. Non-contrast T1- and T2-weighted images were nonspecific, although in our study many lesions showed moderate to markedly high signal on T2-weighted images. All of these investigations reported peripheral ring enhancement on arterial phase images, and in our study, 92 % (12/13) of patients exhibited this on the late arterial phase. Prior reports [21, 23, 24] also observed targetoid appearance on the later post-contrast phases, which also shows different appearances including: (i) a peripheral enhanced rim–outer hypointense band–central-enhancing core or (ii) delayed progressive enhancement towards the centre. This targetoid appearance was present in 69 % (9/13) of our patients and this appearance was not observed in lesions smaller than 2 cm.

Sarcomas excluding angiosarcoma

Prior reports [5, 25] described these lesions as very high signal on T2-weighted images. This feature was also observed in our study and is due to cystic changes of these tumours and/or with large interstitial fluid content [26]. Peripheral mild or diffuse enhancement on the late arterial phase followed by heterogeneous progressive enhancement associated with

septal-like enhancement on the later phases are commonly seen [27], as in our cases, although these features can also be seen in CCAs. The presence of haemorrhage was significant compared to non-sarcomatous other rare primary liver malignancies and this could be a helpful feature for the differentiation, particularly from CCAs. Although haemorrhage is a common finding in hepatic adenomas and HCCs, the presence of typical imaging findings for these tumours such as fat content or washout on post-gadolinium imaging, and clinical findings such as history of oral contraceptive use, chronic liver disease or high alphafetoprotein level can help to exclude rare primary liver tumours.

Angiosarcoma

Progressive nodular enhancement was seen in 50 % (3/6) of patients in our study, which resembled the appearance of haemangiomas concurring in the literature [28–30]. Haemorrhage, which is exceedingly rare in haemangiomas, was detected in 50 % (3/6) of the patients, concurring with prior studies [29, 30]. The presence of haemorrhage was a helpful feature for the diagnosis of AS and was also a commonly detected feature in 53 % (8/15) of other types of sarcomas. Furthermore, the enhancement of haemangioma tends to follow the opacification of large vessels, which is not usually seen in AS [28]. Another key difference is the presence of lobulated margins in virtually all haemangiomas greater than 18 mm [31], which is not usually not seen in AS.

Primary hepatic lymphoma

Variable low T1 and high T2 signal intensities were detected in all cases, similar to previous descriptions [32–35], although mild pre-contrast T1 and T2 signals were also reported as a feature of PHL [33] and this was also noted in some of our patients. Minimal or no enhancement on dynamic post-gadolinium imaging and absence of necrosis in all our cases concur with published literature [35]. A distinctive finding was that tumour masses encased the vessels, rather than deviating them, and this was observed in all our cases.

Despite the presence of helpful diagnostic MRI features, no signs appear to be specific for the diagnosis and differentiation of the rare hepatic primary liver malignancies. However, the lack of typical imaging features of primary neoplasms of the liver should be a clue for the presence of rare primary liver malignancies. Additionally, the lack of strict imaging criteria used for the diagnosis of HCC, such as in the Liver Imaging Reporting and Data System (LI-RADS) reporting system, could be a sign for non-HCC malignancy, as reported recently [16].

A limitation of this study is the relatively few number of cases of each individual malignancy, and we attempted to overcome this limitation by including multiple institutions. Another limitation is that imaging studies were retrospectively reviewed

by investigators at each centre, but not by a central reading site, which might lead to heterogeneity in interpretation of the studies. We attempted to mitigate this error by selecting MRI facilities in which the principal contributor had considerable experience with body MRI (> 10 years' experience at each centre). Another limitation is the use of different equipment, sequences and imaging protocols between institutions; nevertheless these studies were performed with diagnostically accepted standards, which showed minimal variation over time in the last 10 years. The lack of a control group and comparison of the features of these rare primary tumours to the common primary tumours is another limitation; however, we believe this should be the subject of another study.

In conclusion, distinctive MRI features include large heterogeneous central scar in FL, central necrosis and haemorrhage in sarcomas, haemangioma-like enhancement with concurrent haemorrhage in angiosarcomas and encasement of vessels in PHL. The lack of wash-out for all tumour types except mixed HCC-CCA is another important feature of most rare primary hepatic malignancies, while combined features of HCC and CCA are distinctive for mixed HCC-CCA. However, despite the presence of these helpful differential features, histopathological confirmation is usually required for definitive diagnosis.

Funding The authors state that this work has not received any funding.

Compliance with ethical standards

Guarantor The scientific guarantor of this publication is Ersan Altun, M.D.

Conflict of interest The authors of this manuscript declare no relationships with any companies whose products or services may be related to the subject matter of the article.

Statistics and biometry No complex statistical methods were necessary for this paper.

Informed consent Written informed consent was waived by the Institutional Review Boards.

Ethical approval Institutional Review Board approval was obtained.

Methodology

- retrospective
- cross-sectional/observational study
- multicentre study

References

1. Matos AP, Velloni F, Ramalho M, AlObaidy M, Rajapaksha A, Semelka RC (2015) Focal liver lesions: Practical magnetic resonance imaging Approach. *World J Hepatol* 7:1987–2008

2. Braga L, Altun E, Armao D, Semelka RC (2015) Liver. In: Semelka RC, Brown M, Altun E (eds) *Abdominal-pelvic MRI*, 4th edn. Wiley-Blackwell Hooken, NJ, pp 39–393
3. Park JH, Jang KM, Kang TW et al (2016) Identification of imaging predictors discriminating different primary liver tumors in patients with chronic liver disease on gadoteric acid-enhanced MRI: A classification tree analysis. *Eur Radiol* 26:3102–3111
4. Economopoulos N, Kelekis NL, Argentos S et al (2008) Bright-dark sign in MR imaging of hepatic hemangioma. *J Magn Reson Imaging* 27:908–912
5. Crider MH, Hoggard E, Manivel JC (2009) Undifferentiated (Embryonal) Sarcoma of the Liver. *Radiographics* 29:1665–1668
6. LV WF, Han JK, Cheng DL, Tang WJ, Lu D (2015) Imaging features of primary hepatic leiomyosarcoma: A case report and review of literature. *Oncol Lett* 9:2256–2260
7. Chelimilla H, Badipatla K, Ihimoyan A, Niazi M (2013) A Rare Occurrence of Primary Hepatic Leiomyosarcoma Associated with Epstein Barr Virus Infection in an AIDS Patient. *Case Rep in Gastrointestinal Med* 2013:691862. <https://doi.org/10.1155/2013/691862>
8. Wunderbaldinger P, Turetschek K (1998) Primary Malignant Fibrous Histiocytoma of the Liver: CT and MR Findings. *Am J Roentgenol* 171:900–901
9. Sunnapwar A, Katre R, Poicarpio-Nicolas M, Katabathina V, Erian M (2016) Imaging of rare primary malignant hepatic tumors in adults with histopathologic correlation. *J Comp Assist Tomogr* 40:452–462
10. Tan Y, Xiao E-H (2013) Rare hepatic malignant tumors: dynamic CT, MRI, and clinicopathologic features: with analysis of 54 cases and review of the literature. *Abdom Imaging* 38:511–526
11. Goodman ZD, Ishak KG, Langloss JM et al (1985) Combined hepatocellular-cholangiocarcinoma. A histologic and immunohistochemical study. *Cancer* 55:124–135
12. Theise ND, Nakashima O, Park YN, Nakanuma Y (2010) Combined hepatocellular carcinoma-cholangiocarcinoma. WHO classification of tumours of the digestive system, 4th edn. IARC Press, Lyon
13. Fowler KJ, Sheybani A, Parker RA et al (2013) Combined Hepatocellular and Cholangiocarcinoma (Biphenotypic) Tumors: Imaging Features and Diagnostic Accuracy of Contrast-Enhanced CT and MRI. *Am J Roentgenol* 201:332–339
14. Maximina S, Ganeshane DM, Shanbhogued AK et al (2014) Current update on combined hepatocellular-cholangiocarcinoma. *Eur J of Radiol Open* 1:40–48
15. de Campos RO, Semelka RC, Azevedo RM et al (2012) Combined Hepatocellular Carcinoma-Cholangiocarcinoma: Report of MR Appearance in Eleven Patients. *J Magn Reson Imaging* 36:1139–1147
16. Potretzke TA, Tan BR, Doyle MB, Brunt EM, Heiken JP, Fowler KJ (2016) Imaging features of biphenotypic primary liver carcinoma (hepatocholangiocarcinoma) and the potential to mimic hepatocellular carcinoma: LIRADS analysis of CT and MRI features in 61 cases. *AJR* 207:25–31
17. Kim R, Lee JM, Shin C-I et al (2016) Differentiation of intrahepatic mass-forming cholangiocarcinoma from hepatocellular carcinoma on gadoteric acid-enhanced liver MR imaging. *Eur Radiol* 26:1808–1817
18. Ganeshan D, Szklaruk J, Kundra V, Rashid AK, Elsayes KM (2014) Imaging Features of Fibrolamellar Hepatocellular Carcinoma. *Am J Roentgenol* 202:544–552
19. Smith MT, Blatt ER, Paul Jedlicka P, Strain JD, Fenton LZ (2008) Fibrolamellar Hepatocellular Carcinoma. *Radiographics* 28:609–613
20. Ichicava T, Federle MP, Grazioli L, Madariaga J, Nelesnik M, Marsh W (1999) Fibrolamellar hepatocellular carcinoma: Imaging and pathologic findings in 31 recent cases. *Radiology* 213:352–361
21. Paolantonio P, Laghi A, Vanzulli A et al (2014) MRI of Hepatic Epithelioid Hemangi endothelioma (HEH). *J Magn Reson Imaging* 40:552–558
22. Lin J, Ji Y (2010) CT and MRI diagnosis of hepatic epithelioid hemangi endothelioma. *Hepatobiliary Pancreat Dis Int.* 9:154–158
23. Gan L, Chang R, Jin H, Yang L (2016) Typical CT and MRI signs of hepatic epithelioid hemangi endothelioma. *Oncol Lett* 11:1699–1706
24. Giardino A, Miller FH, Kalb B et al (2016) Hepatic epithelioid hemangi endothelioma: a report from three university centers. *Radiol Bras* 49:288–294
25. Iqbal K, Xian ZM, Yuan C (2008) Undifferentiated liver sarcoma – rare entity: a case report and review of the literature. *J Medical Case Rep* 2:20
26. Tsukada A, Ishizaki Y, Nobukawa B, Kawasaki S (2010) Embryonal Sarcoma of the Liver in an Adult Mimicking Complicated Hepatic Cyst: MRI Findings. *J Magn Reson Imaging* 31:1477–1480
27. Yu R-S, Chen Y, Jiang B, Wang L-H, Xu X-F (2008) Primary hepatic sarcomas: CT findings. *Eur Radiol* 18:2196–2205
28. Thapar S, Rastogi A, Ahuja A, Sarin S (2014) Angiosarcoma of the liver: imaging of a rare salient entity. *J Radiol Case Rep* 8:24–32
29. Kumasaka S, Okauchi K, Taketomi AT, et al. (2014) Angiosarcoma: Review of CT and MR Imaging features. Abstract. European Congress of Radiology Meeting
30. Koyama T, Fletcher JG, Johnson CD et al (2002) Primary Hepatic Angiosarcoma: Findings at CT and MR Imaging. *Radiology* 222:667–673
31. Matos AP, Jeon YH, Ramalho M, AlObaidy M, Semelka RC (2016) Lobulated margination of liver hemangiomas: Is this a definitive feature? *Clin Imaging* 40:801–805
32. Rajesh S, Bansal K, Sureka B, Patidar Y, Bihari C, Arora A (2015) The imaging conundrum of hepatic lymphoma revisited. *Insights Imaging* 6:679–692
33. Maher MM, Mcdermott SR, Fenlon HM et al (2001) Imaging of Primary Non-Hodgkin's Lymphoma of the Liver. *Clinical Radiology* 56:295–301
34. Steller EJA, Leeuwen MSV, Hillegersberg RV et al (2012) Primary lymphoma of the liver: A complex diagnosis. *World J Radiol* 4:53–57
35. Kelekis NL, Semelka RC, Siegelman ES et al (1997) Focal hepatic lymphoma: Magnetic resonance demonstration using current techniques including gadolinium enhancement. *Magn Reson Imaging* 15:625–636